Published in final edited form as:
J Innate Immun. 2013 ; 5(2): 124–136. doi:10.1159/000342430.

Francisella tularensis alters human neutrophil gene expression: insights into the molecular basis of delayed neutrophil apoptosis

Justin T. Schwartz[a,b,1], **Sarmistha Bandyopadhyay**[a,c,1], **Scott D. Kobayashi**[d], **Jenna McCracken**[a,b], **Adeline R. Whitney**[d], **Frank R. DeLeo**[d], and **Lee-Ann H. Allen**[a,b,c,2]

[a]Inflammation Program, University of Iowa and the Veteran's Administration Medical Center, Iowa City, IA 52242

[b]Department of Microbiology, University of Iowa and the Veteran's Administration Medical Center, Iowa City, IA 52242

[c]Department of Internal Medicine, University of Iowa and the Veteran's Administration Medical Center, Iowa City, IA 52242

[d]Laboratory of Human Bacterial Pathogenesis, Rocky Mountain Laboratories, National Institute of Allergy and Infectious Diseases, National Institutes of Health, Hamilton, MT 59840

Abstract

We demonstrated recently that *Francisella tularensis* profoundly impairs human neutrophil apoptosis, but how this is achieved is largely unknown. Herein we used human oligonucleotide microarrays to test the hypothesis that changes in neutrophil gene expression contribute to this phenotype, and now demonstrate that *F. tularensis* live vaccine strain (LVS) caused significant changes in neutrophil gene expression over a 24 h time period relative to the uninfected controls. Of ~47,000 genes analyzed, 3,435 were significantly up- or down-regulated by LVS, including 365 unique genes associated with apoptosis and cell survival. Specific targets in this category included genes associated with the intrinsic and extrinsic apoptotic pathways (*CFLAR*, *TNFAIP3*, *TNFRSF10D*, *SOD2, BCL2A1*, *BIRC4*, *PIM2*, *TNFSF10*, *TNFRSF10C*, *CASP2*, and *CASP8*) and genes that act via the NF B pathway and other mechanisms to prolong cell viability (*NFKB1*, *NFKB2*, and *RELA*, *IL1B*, *CAST, CDK2, GADD45B*, *BCL3*, *BIRC3*, *CDK2*, *IL1A*, *PBEF1*, *IL6*, *CXCL1*, *CCL4* and *VEGF*). The microarray data were confirmed by qPCR and pathway analysis. Moreover, we demonstrate that X-linked inhibitor of apoptosis (XIAP) protein remained abundant in PMNs over 48 h of LVS infection, whereas BAX mRNA and protein were progressively down-regulated. These data strongly suggest that antiapoptotic and pro-survival mechanisms collaborate to sustain the viability of *F. tularensis* infected neutrophils.

[2]Corresponding author information: Lee-Ann H. Allen, Ph.D., Inflammation Program, University of Iowa, 2501 Crosspark Rd., MTF D-154, Coralville, IA 52241, Phone: 319-335-4258, Fax: 319-335-4194, lee-ann-allen@uiowa.edu.
[1]JTS and SB contributed equally to this study

Conflicts of interest
None.

Author contributions
J.T.S. designed and performed experiments, interpreted data and co-wrote the manuscript. S.B., S.D.K., J.M. and A.R.W. designed and performed experiments, interpreted data and edited the manuscript. F.R.D. designed experiments, interpreted data and edited the manuscript. L.-A.H.A. designed experiments, interpreted data and co-wrote the manuscript.

Keywords

neutrophil; polymorphonuclear leukocyte; apoptosis; gene expression; microarray; tularemia; XIAP; BAX

Introduction

Polymorphonuclear leukocytes (PMNs) are short-lived cells that are critical for innate host defense and utilize a combination of NADPH oxidase-derived reactive oxygen species (ROS), antimicrobial peptides and degradative enzymes to kill engulfed microorganisms [1]. Moreover, timely apoptosis and clearance of effete neutrophils are also essential for resolution of the inflammatory response [2–5]. As components of the PMN killing arsenal are synthesized during cell development and packaged into cytoplasmic granules that cannot be replenished, it was previously believed that mature neutrophils were nearly transcriptionally inert and synthesized few proteins [5,6]. However, with the advent of systems biology approaches it became apparent that neutrophil lifespan is in part regulated at the transcriptional level, and that constitutive turnover of these cells requires specific changes in gene expression that comprise an 'apoptosis differentiation program' [2,3,5,7,8]. Since the seminal studies of Watson [9] it has been apparent that phagocytosis of most bacteria and other particles dramatically accelerates neutrophil apoptosis relative to unstimulated controls, and recent studies indicate that additional oxidant-dependent changes in gene expression are required for this 'phagocytosis-induced cell death' (PICD) response [5,7,8,10–12].

Francisella tularensis is a facultative intracellular bacterium that infects many cell types including neutrophils. As virulent *F. tularensis* strains require Biosafety Level-3 containment, an attenuated live vaccine strain (LVS) is often utilized as a model organism for tularemia research. LVS does not cause disease in humans, but maintains virulence in mice and demonstrates similar phenotypes to virulent *F. tularensis* strains during *in vitro* infection of human phagocytes [13–15]. *F. tularensis* is not killed by human or rhesus monkey PMNs [13–16], and we have shown that this is due to inhibition of the respiratory burst followed by phagosome escape and bacterial replication in the cytosol [13–15]. In addition, we recently demonstrated using biochemical approaches that neither LVS nor the virulent *F. tularensis* strain Schu S4 triggers PICD [15]. Instead, these organisms significantly inhibit constitutive as well as FAS-triggered PMN apoptosis and profoundly prolong cell lifespan [15]. We hypothesized that this phenotype may be manifest at the level of gene expression, and demonstrate here that *F. tularensis* LVS induced a transcriptional response in human PMNs that is characterized by downregulation of proapoptotic factors and induction of anti-apoptosis and pro-survival genes.

Materials and Methods

Materials

Cysteine heart agar was obtained from Becton, Dickinson and Company (Sparks, MD). Defibrinated sheep blood was from Remel (Lenexa, KS). Endotoxin-free Dulbecco's PBS, Hank's buffered saline solution (HBSS), and HEPES buffer were from Mediatech Incorporated (Herndon, VA). Clinical grade dextran (m.w. 500,000 Da) was purchased from Pharmacosmos A/S (Holbaek, Denmark). Ficoll-Paque Plus was obtained from GE Healthcare Bio-sciences (Uppsala, Sweden). Endotoxin-free HEPES-buffered RPMI-1640 medium was from Lonza (Walkersville, MD). Protocol HEMA-3 staining kit was purchased from Fisher Scientific (Kalamazoo, MI). Annexin V-FITC conjugate was obtained from Invitrogen (Camarillo, CA). Rabbit anti-*F. tularensis* antiserum and anti-XIAP monoclonal

antibodies (mAbs) were from BD Diagnostics (Sparks, MD). Anti-BAX mAb clone 6A7 was from Sigma-Aldrich (St. Louis, MO). Mouse anti-actin mAb (clone JLA20) was from Calbiochem (Darmstadt, Germany). DyLight™ 549-conjugated donkey-anti-rabbit F(ab')$_2$ secondary Ab was from Jackson ImmunoResearch Laboratories (West Grove, PA). Horseradish peroxidase-conjugated antibodies were from Bio-Rad Laboratories (Hercules, CA). DAPI, and Pierce BCA protein assay kits and SuperSignal West Pico Enhanced Chemiluminescence substrate regents were from Thermo Scientific (Rockford, IL). RLT buffer was from Qiagen (Valencia, CA). Human HU133 Plus 2.0 oligonucleotide microarrays were from Affymetrix (Santa Clara, CA).

Cultivation of bacteria and opsonization

F. tularensis subspecies *holarctica* live vaccine strain (LVS) (ATCC 29684) was inoculated onto cysteine heart agar supplemented with 9% defibrinated sheep blood and grown for 48 h at 37°C in 5% CO_2. Bacteria were harvested from the plates, washed twice with HBSS (containing Ca^{2+} and Mg^{2+}), and quantified by measurement of absorbance at 600 nm. Serum opsonization was performed by incubating *F. tularensis* LVS (1×10^{10}/ml) or yeast zymosan particles in 50% pooled human serum for 30 min at 37°C, followed by two washes with HBSS prior to infection of PMNs.

Neutrophil isolation

Heparinized venous blood was obtained from healthy adult volunteers in accordance with a protocol approved by the Institutional Review Board for Human Subjects at the University of Iowa. PMNs were isolated using dextran sedimentation followed by density gradient separation as previously described [17]. PMNs were suspended in HBSS without divalent cations, counted, and diluted to 2×10^7/ml. Purity of the PMN preparations was assessed by HEMA-3 staining followed by microscopic analysis, and the suspensions were routinely 95–98% neutrophils and 2–5% eosinophils.

Infection of human neutrophils with *F. tularensis* LVS or opsonized zymosan

Infections of human neutrophils with LVS were performed as previously described [15]. Briefly, PMNs (5×10^6/ml) were diluted in HEPES-buffered RPMI-1640 medium (without serum) and mixed with *F. tularensis* LVS at multiplicity of infection (MOI) 200:1. One milliliter aliquots of each suspension were transferred into 5 ml polypropylene tubes and subsequently incubated at 37°C with 5% CO_2 for 0–48 h. Notably, the samples used for microarray analysis were simultaneously processed for microscopy, Annexin V-staining and RNA preparation (see below). Where noted, PMNs were stimulated in a similar manner with opsonized zymosan (OpZ) at MOI 5:1.

Immunofluorescence microscopy

At the indicated time points, an aliquot of PMNs was washed twice with cold PBS and cyto-centrifuged onto acid-washed coverslips. Cells were fixed with 10% formalin, permeabilized in cold (1:1) methanol-acetone, and blocked in PBS supplemented 0.5 mg/ml NaN_3 and 5 mg/ml BSA using our established methods [15]. LVS was detected using anti-*F. tularensis* antiserum and DyLight™ 549-conjugated donkey-anti-rabbit F(ab')$_2$ secondary antibodies, and DAPI was used to stain PMN nuclei. The infection efficiency (percentage of PMN with ≥1 bacterium) and association index (mean number of bacteria per cell) were determined by counting 300 PMNs per coverslip using epifluorescence microscopy. Confocal images were obtained using a Zeiss LSM 710 confocal microscope and Zen imaging software (Carl Zeiss, Inc., Thornwood, NY).

Detection of neutrophil apoptosis using Annexin V

Neutrophil apoptosis was assessed by measuring phosphatidylserine (PS) externalization on the PMN surface using Annexin V as we described [15] with propidium iodide staining included to distinguish early apoptotic cells from late apoptotic/necrotic PMNs. In brief, PMNs (5×10^6/ml) were left untreated or infected with LVS in suspension as described above. An aliquot of PMNs was removed at the indicated time points and subsequently co-stained with Annexin V-FITC and propidium iodide in Annexin V binding buffer (10 mM HEPES/NaOH, pH 7.4, 140 mM NaCl, 2.5 mM $CaCl_2$) prior to analysis using a FACSCalibur flow cytometer (Becton Dickson). Twenty thousand events were collected for each sample and the data were analyzed using CellQuest (Becton Dickson) and FlowJo software (Tree Star, Inc.).

RNA preparation and analysis of human neutrophil gene expression using microarrays

PMNs (1×10^7) were left untreated or infected with LVS in suspension as described above. Experiments were performed using cells from four independent donors on different days. At the designated time points, neutrophils were pelleted and then lysed directly using RLT buffer. Time zero samples were processed immediately after addition of LVS or an equivalent volume of medium to the cells without further incubation at 37°C. Purification of neutrophil RNA and subsequent preparation of labeled cRNA was performed as previously described [8,18]. Labeling of samples, hybridization of cRNA to Affymetrix HU133 Plus 2.0 oligonucleotide arrays, and scanning were performed according to Affymetrix protocols as described (http://www.affymetrix.com/pdf/expression_manual.pdf). A separate oligonucleotide array was utilized for each donor at each time point.

The microarray data were analyzed using a standard method that has been published many times [18]. In brief, a preliminary analysis of the raw microarray data was performed using Affymetrix GeneChip Operating Software (GCOS v1.4) to generate scaled data in numerical format. These data were imported into Partek Genomics Suite software (Partek Inc., St. Louis, Missouri) and a principal components analysis (PCA) was performed to visualize variance in the data. Microarray data from unstimulated and stimulated PMNs were normalized in Partek and analyzed using ANOVA and false discovery rate (FDR) controls to correct for multiple comparisons. Genes from PMNs stimulated with *F. tularensis* LVS were initially defined as differentially expressed compared to unstimulated PMNs if they were statistically significant by ANOVA and FDR at the level of $P<0.05$ and were increased or decreased at least 2-fold. In addition, transcripts had to have a scaled expression value of at least 500 in one of the two groups (unstimulated or stimulated). For down-regulated genes, transcripts must have been called present or marginal in 3 of 4 unstimulated PMN RNA samples; for up-regulated genes, transcripts must have been called present or marginal in 3 of 4 *F. tularensis*-stimulated PMN RNA samples. Genes that met the criteria for significant differential expression are provided in online Supplemental Table 1, and a complete set of microarray data are posted on the Gene Expression Omnibus (GEO, http://www.ncbi.nlm.nih.gov/geo/accession number GSE37416).

Differentially expressed genes were further analyzed to identify the associated pathways using Database for Annotation, Visualization and Integrated Discovery (DAVID) v6.7 bioinformatics software [19,20] and MetaCore analysis software (GeneGo Inc., Minneapolis, MN). The differentially expressed genes were classified in gene ontology (GO) categories using DAVID based on their potential biological roles. The GO classification was based on the GO-BP-FAT format.

Real time PCR confirmation of microarray data

Total RNA was isolated using TRIzol (Invitrogen Life Technologies, Grand Island, NY) according to the manufacturer's instructions and RNA concentrations were measured by Nanodrop ND-1000 spectrophotometry. All experiments for real time PCR analysis were performed using conditions identical to those used for the microarray experiments (described above). RNAs were analyzed using an ABI 7000 thermocycler (Applied Biosystems, Life Technologies, CA). Primers were designed using the Primer Express program (Applied Biosystems) and obtained from Integrated DNA technologies (Coralville, IA). To analyze gene expression, 240 ng of total RNA was reverse transcribed using multiscribe reverse transcriptase and then amplified with gene-specific primers using SYBR Green PCR master mix (Applied Biosystems Life Technologies, Grand Island, NY). Melting curve analysis was used to check product specificity. The relative expression level of each transcript was normalized to glyceraldehyde 3-phosphate dehydrogenase.

Immunoblotting

At the desired time points PMNs were pelleted, resuspended in ice-cold protease and phosphatase inhibitor cocktail (Tris-buffered saline containing aprotinin, leupeptin, phenylmethylsulfonyl fluoride, sodium orthovanadate, 4-(2-aminoethyl) benzenesulfonyl fluoride hydrochloride, levamisole, bestatin, E-64, and pepstatin A), and incubated on ice for 10 min. PMNs were lysed by addition of NP-40 to 1% final concentration, and lysates were clarified by centrifugation. Protein concentrations of the clarified lysates were determined using the Pierce BCA Protein Assay. Ten to 20 g of each clarified lysate were separated using NuPAGE 4–12% Bis-Tris gradient gels and then transferred to polyvinylidene fluoride membranes. Blocked membranes were probed to detect XIAP, BAX, or actin. Bands were detected using horseradish peroxidase-conjugated secondary antibodies and Pierce Supersignal West Pico Enhanced Chemiluminescence reagents.

Statistical Analysis

As noted above, microarray data were analyzed using three-way ANOVA [8,18]. Spearman correlation analysis was used to compare the microarray and qPCR results, and both the correlation coefficient (r) and *P* value are reported. For other experiments, multiple sample groups were compared using two-way ANOVA with Tukey's post-test, and studies with one control and one treatment group were evaluated using an unpaired two-sided Student *t* test.. Unless otherwise indicated, analyses were performed using GraphPad Prism v4.0 software. $P<0.05$ was considered statistically significant.

Results

F. tularensis LVS delays spontaneous apoptosis of human neutrophils

We previously demonstrated that both LVS and the virulent *F. tularensis* strain Schu S4 inhibit constitutive neutrophil apoptosis and thereby prolong neutrophil lifespan [15]. As both neutrophil apoptosis and proinflammatory capacity are regulated in part at the transcriptional level [3,5,7,8,10], we evaluated global gene expression in human PMNs during infection with *F. tularensis* LVS. To this end, neutrophils from four different donors were infected with LVS in suspension in serum-free RPMI-1640 medium, an established approach for studies of neutrophil apoptosis that avoids confounding effects of growth factors and other serum components on cell viability [21,22]. At each time point, samples were processed to quantify infection efficiency and the extent of apoptosis in the same samples that were used for RNA extraction and microarray analysis. As we reported previously [15], uptake of *F. tularensis* is inefficient under these conditions and an MOI of 200:1 was used to ensure that most PMNs were infected (Fig. 1A–B). By 6 h, approximately

65% of neutrophils contained 1–2 bacteria each, and over the time course examined both the percentage of infected PMNs and the bacterial load per cell increased progressively. Thus, by 24 h the majority of neutrophils exhibited high bacterial burdens (Fig. 1A–B). In addition, we confirmed the ability of LVS to prolong PMN viability over 48 h post-infection using Annexin V-FITC staining and flow cytometry analysis to detect PS exposed on the surface of apoptotic cells. Relative to untreated controls, LVS profoundly diminished PMN apoptosis at 12, 24 and 48 h (Fig. 1C), confirming published data [15]. These results set the stage for our microarray studies, and in this regard it is noteworthy that under these conditions both extracellular and intracellular LVS contribute to the ability of this bacterium to extend PMN lifespan [15].

F. tularensis LVS induces global changes in PMN gene expression

To gain insight into the molecular mechanisms that account for the ability of *F. tularensis* to modulate PMN function we performed microarray studies to screen ~47,000 human genes for changes in expression at 0, 3, 6, 12, 24 and 48 h, and in each case control and LVS-treated PMN were directly compared. As noted above, RNA samples were prepared on different days using neutrophils from four individual healthy donors, and each sample was analyzed on a separate gene chip.

We used PCA mapping (Fig. 2A) first to reduce mathematically the dimensionality of the spectrum of gene expression values, and obtain information regarding the total amount of variation within the dataset [23,24]. Our data show that the control and LVS-stimulated PMNs clustered together at 0 h, which suggests similarity between the initial data sets and demonstrates that initial mixing of LVS and PMNs did not in and of itself alter the PMN transcriptome. In marked contrast, the transcriptional profiles of the LVS-treated cells clearly segregated from the uninfected control PMNs as infection progressed, with distinctions between these groups apparent by 3 h, and more profound differences detected at 6, 12, 24 and 48 h. As many of the control PMNs had progressed to late apoptosis/secondary necrosis by 48 h, this limited the utility of this data set, and we included only the 0–24 h data in our subsequent analyses.

Next, we used criteria described in detail in the *Methods* to analyze the microarray data and identified 3,435 genes (1,149 induced and 2,286 repressed) that were significantly ($P<0.05$) differentially regulated during LVS infection over 3–24 h (see online Supplemental Table 1, which contains all of the significantly differentially expressed genes identified in these experiments). Consistent with the PCA, we observed that the number of genes differentially expressed during infection increased over time, with only 125 genes induced or repressed at 3 h, and 2,916 genes differentially regulated at 24 h (Fig. 2B).

To validate the microarray data, we selected eight differentially expressed genes for confirmation by quantitative real-time RT-PCR. We included four significantly up-regulated genes and four significantly down-regulated genes that were representative of the range of responses obtained on the microarrays, and also known to be associated with modulation of apoptosis (*MIF, CDKN1A, SOD2, TNFSF10, MCL1*), cell survival (*DDIT4*) or the inflammatory response (*F2RL1, FGL2*) (Fig. 2C). Statistical analysis revealed a strong positive correlation (Spearman correlation coefficient $r = 0.90$, $P=0.0046$) between the oligonucleotide microarray and the qPCR results (Fig. 2C, *inset*).

Apoptosis pathways are significantly modulated during LVS infection

To identify pathways relevant to *F. tularensis* infection, we utilized DAVID [19,20] and Metacore GeneGo software to map our list of differentially expressed genes at 3, 6, 12, and 24 h to predefined pathways in two separate pathway databases, Kyoto Encyclopedia of

Genes and Genomes (KEGG; Kanehisa Laboratories, Kyoto University, Kyoto, Japan) and Metacore GeneGo. KEGG is a database of approximately 250 canonical signaling, metabolic, and disease pathways, whereas the MetaCore software utilizes a proprietary, manually curated database of approximately 450 pathways involved in protein-protein, protein-DNA, and protein-compound interactions as well as metabolic and signaling pathways. Twenty-seven different KEGG pathways were identified by DAVID to be significantly enriched in differentially expressed genes between 3–24 h (Table 1), and 11 unique pathways were involved in apoptosis or cellular survival (Table 1, *asterisks*). Of note, the apoptosis pathway was identified as significantly enriched at all time points, and was highly significant at 6 and 12 h (P=0.002 and 0.00038, respectively). Consistent with the DAVID pathway analysis, five of the top 10 most significant GenGo pathways were involved in apoptosis and cell survival (Fig. 3, *asterisks*). Of these five pathways, two were specifically involved in apoptosis (Fig. 3, *green shading*). Collectively, these data strongly suggest that neutrophil survival during *F. tularensis* infection is modulated, at least in part, by changes in neutrophil gene expression.

Genes involved in apoptosis and cell survival are differentially regulated in PMNs during LVS infection

To facilitate subsequent analysis of the dataset, the differentially expressed genes identified between 3–24 h were divided into functional categories using gene ontology classification by DAVID (GO-BP-FAT format). As in other studies [10,25], we further classified the functional categories into five groups associated with various biological functions: apoptosis and cell survival; transcription, translation, and DNA binding; metabolism; host defense and signal transduction; and vesicle transport and protein localization (Fig. 4). Although the main objective of this study is to gain insight into the molecular mechanisms of prolonged neutrophil survival during LVS infection, many genes in other categories also exhibited significant differential expression. Of particular interest are several Rab family GTPases that regulate membrane trafficking (*RAB1A, RAB5C, RAB7A, RAB8B, RAB9A, RAB20, RAB21* and *RAB33A*) and peroxisome biogenesis factors (*PEX1, PEX12, PEX13, PEX19* and *PEX26*), as well as enzymes involved in signaling and host defense including certain protein kinase C (*PRKCB*) and phosphatidylinositol 3-kinase (*PI3KCB*) isoforms, cyclic AMP-dependent protein kinase, MAP kinases, phosphatases, and components of the ubiquitin conjugation machinery (*UBE2VIP, TMEM189-UB, TMEM189*, and *Ube2v1*) (Supplemental Table 1).

In total, 365 unique genes implicated in apoptosis or cellular survival were significantly differentially regulated between 3 and 24 h post-infection. Depicted in Figure 5 are genes in this category that have been shown to be modulated in other studies of neutrophil apoptosis induction or inhibition, genes recently linked to apoptosis or cell survival (such as *CAST*), and a few genes that may be selectively affected by LVS (such as *AIM2*). Of note, several anti-apoptosis genes, including *TNFAIP3*, *TNFAIP8*, *TNFRSF10D*, *CFLAR*, *BCL2A1*, *PIM2*, and *BIRC4*, were significantly up-regulated in PMNs between 6 and 24 h after infection with LVS. Proteins encoded by these genes inhibit apoptosis signaling at multiple steps in both the extrinsic (*CFLAR*, *TNFAIP3*, *TNFRSF10D*, *SOD2*) and intrinsic (*BCL2A1*, *BIRC4*, *PIM2*, *BIRC3*) pathways. Conversely, several genes involved in inducing apoptosis were repressed during infection, including *TNFSF10*, *TNFRSF10C*, *CASP2*, and *CASP8*.

In addition to genes specifically linked to apoptosis, a number of genes involved in pro-survival responses were also identified. Genes encoding cytokines (*IL1B*, *IL1A*, *PBEF1*, *IL6*), chemokines (*CXCL1*, *CCL4*), and growth factors (*VEGF*) were among the genes up-regulated by LVS, and the encoded proteins have been shown to suppress neutrophil apoptosis *in vitro* [26–28]. The NFκB pathway controls expression of several pro-survival

proteins in neutrophils, and as such is an important regulator of cell lifespan [2]. Both genes involved in NFκB signaling (*NFKB1*, *NFKB2*, and *RELA*) and known NFκB-regulated target genes (*IL1B*, *TRAF1*, *SOD2*, *GADD45B*, *CFLAR*, *TNFAIP3*, *BCL2A1*, *BCL3*, *BIRC3*, and *BIRC4*) linked to cell survival were significantly upregulated by LVS. These data suggest that LVS may promote neutrophil survival in part by stimulating the NFκB pathway. Furthermore, it has been recently suggested that the cyclin-dependent kinases (CDKs) play a critical and previously unappreciated role in regulation of neutrophil apoptosis [2,29]. *CDK2* was among the first set of genes induced by LVS (2.4 fold at 3-h, 4.2 fold at 12 h, and 5.2 fold at 24 h), and *CDK7* was also upregulated. Whether these or other CDK isoforms affect PMN lifespan during *F. tularensis* infection is as yet unknown.

Calpains are cytosolic cysteine proteases that participate in initiation of spontaneous and FAS-mediated neutrophil apoptosis [30]. In healthy cells calpain activity is inhibited by its association with calpastatin. During apoptosis, calpastatin is degraded, which frees calpain to activate BAX and to degrade the potent caspase inhibitor XIAP [2,29,30]. *CAST*, which encodes calpastatin, was upregulated 4-fold at 12 h and 9-fold at 24 h by LVS. Therefore, stabilization or up-regulation of calpastatin levels in neutrophils during LVS infection may enhance PMN survival by inhibiting the proapoptotic function of the calpain proteases.

BAX expression is diminished in LVS-infected PMNs, and proinflammatory capacity is sustained

BAX is a proapoptotic member of the BCL-2 family that controls release of cytochrome *c* from mitochondria. *BAX* is induced in PMNs by phagocytosis of bacteria or other particles in a ROS-dependent manner [7,8,10], and is considered a hallmark of the PICD pathway. Consistent with this, BAX mRNA (Fig. 6A) and protein (Fig. 6B) were transiently elevated in OpZ-stimulated PMNs. In stark contrast, *BAX* mRNA declined progressively 3–24 h after infection with LVS (Fig. 6A), and BAX protein in neutrophil lysates appeared diminished at 12 and 24 h as compared with the actin loading control (Fig. 6B). Downregulation of BAX may synergize with diminished ROS production to prevent PICD, and likely contributes to the ability of *F. tularensis* to prolong PMN lifespan.

During apoptosis PMN proinflammatory capacity is strongly down-regulated [1,3]. Thus, when apoptosis is impaired neutrophils exhibit a sustained proinflammatory phenotype. Consistent with this, expression of several proinflammatory genes was enhanced by LVS including *VEGF*, *IL1B*, *IL6* and *CXCL1* (Fig. 5) as well as *OSM* and *IL1RN* (Supplemental Table 1). In contrast, *IL8* was unaffected (data not shown), results consistent with the fact that CXCL8 is not secreted by PMNs infected with live *F. tularensis* [15].

LVS-infected neutrophils contain large amounts of the antiapoptotic protein XIAP

Our published data indicate that both proenzyme processing and the activity of mature caspases-9 and -3 are profoundly diminished and delayed by *F. tularensis* [15], but what accounts for this is unclear. XIAP is a member of the inhibitor of apoptosis protein family that directly inhibits the activity of caspase-9 and -3, and also inhibits processing of the respective procaspases to their mature forms [2,31]. As the genes that encode calpastatin (*CAST*) and to a lesser extent XIAP (*BIRC4*) were upregulated by LVS (Fig. 5), we hypothesized that XIAP protein may be elevated or sustained in infected PMNs. To test this, immunoblots prepared using control and LVS-infected PMN lysates were probed with XIAP-specific antibodies. By this assay, XIAP (57 kDa) declined precipitously in the uninfected control PMN at time points >12 h after isolation, with concomitant accumulation of a ~30kDa calpain cleavage fragment (Fig. 7), confirming published data [32]. In stark contrast, XIAP remained abundant in LVS-infected PMNs, and only very small amounts of the p30 XIAP fragment were detected over the time course examined (Fig. 7). These data

strongly suggest that maintenance of XIAP at high levels is one mechanism used by *F. tularensis* to diminish caspase activity and impair PMN apoptosis.

Discussion

We recently demonstrated that *F. tularensis* impairs spontaneous neutrophil turnover as well as apoptosis triggered by FAS crosslinking [15], but how this is achieved is largely unknown. Upon discovery of the apoptosis differentiation program, it became apparent that neutrophil turnover is regulated at the transcriptional level, and that apoptosis is a final, regulated stage of the neutrophil lifecycle that is subject to manipulation by bacterial pathogens [5,7,11,12]. In keeping with this, the results of this study demonstrate that *F. tularensis* LVS alters the human neutrophil transcriptome, including expression of genes associated with apoptosis and cell fate. Collectively, our data suggest that changes in expression of key pathway components and regulatory factors, as well as pro-survival signaling intermediates and cytokines, may act in concert to profoundly prolong PMN lifespan during *F. tularensis* infection.

Neutrophil apoptosis can be initiated by the extrinsic (death receptor) or intrinsic (mitochondrial) pathways (see model in Fig. 8). The extrinsic pathway is triggered by ligation of surface death receptors (FAS, tumor necrosis factor receptor-1 (TNFR1), and tumor necrosis factor-related apoptosis-inducing ligand (TRAIL)) [2,29], which leads to formation of a death-inducing signaling complex at the membrane that is required for activation of procaspase-8. On the other hand, the intrinsic pathway is triggered by disruption of the outer mitochondrial membrane, which leads to activation of procaspase-9, and is the dominant pathway involved in constitutive neutrophil turnover [5]. The results of this study indicate that multiple genes known to regulate apoptosis signaling via these pathways were differentially expressed in response to LVS (Figs. 5 and 8). In particular, several extrinsic pathway antagonists and inhibitors were significantly upregulated including *CFLAR*, *TNFAIP3*, *SOD2* and *TNFRSF10D*, whereas proapoptotic factors in this pathway, including TRAIL (*TNFSF10*) and caspase-8 (*CASP8*), were down-regulated. LVS also induced expression of several antiapoptotic genes in the intrinsic pathway, including *BCL2A1*, *BIRC4, BIRC3* and *PIM2*. XIAP and cIAP (encoded by *BIRC4* and *BIRC3*, respectively) act directly on caspases to diminish cell death [2,29,31]. PIM2 is a serine/threonine kinase that inhibits apoptosis by phosphorylating BAD [33]. In addition, *BCL2A1* encodes BFL-1, an antiapoptotic BCL-2 family protein that inhibits crosstalk between the extrinsic and intrinsic pathways by interacting with and sequestering tBID [34] (Fig. 8).

Regulation of mitochondrial integrity is a central control point in apoptosis that is governed by the balance of pro- and anti-apoptotic BCL-2 family members [2,29]. In healthy PMNs anti-apoptotic BCL-2 proteins (MCL-1, A1 and BCL-XL) are present in excess relative to BAX and BAK and sequester these proapoptotic proteins in the cytosol to preserve mitochondrial integrity. During constitutive apoptosis, expression of antiapoptotic BCL-2 proteins declines selectively. This allows BAX/BAK oligomers to form pores in the outer mitochondrial membrane that in turn permit translocation of cytochrome *c* from the intermembrane space to the cytosol for initiation of apoptosome formation and caspase-9 activation (Fig. 8). Rapid ROS-dependent induction of *BAX* markedly accelerates neutrophil apoptosis, and this is a hallmark of the PICD pathway [10]. VDAC is a voltage-dependent anion channel in the outer mitochondrial membrane that also contributes to organelle integrity. We demonstrated previously that *F. tularensis* uncouples phagocytosis from NADPH oxidase activation [13,14], and show here that expression of *BAX* mRNA and protein were significantly diminished (Fig. 6), whereas expression of *VDAC* was enhanced (Fig. 5). These data account for the fact that *F. tularensis* does not trigger PICD, and also suggest that differential effects of this organism on *BAX* and *VDAC* may sustain

mitochondrial integrity during infection. Additional studies of mitochondrial structure and BAX localization during *F. tularensis* infection are therefore warranted.

Calpains and the proteasome are essential for constitutive PMN apoptosis [34], and calpain inhibitors prevent proteasome-mediated degradation of XIAP and MCL-1 in a protein kinase A-dependent manner [35]. We show here that genes encoding several proteasome subunits (*PSMA2*, *PSMA3*, *PSMB2*, *PSME3*, *PSMB6*, *PSMB4*, *PSMB7*, *PSMD1* and *PSMD6*) were down-regulated by LVS, whereas expression of the calpain inhibitor calpastatin (*CAST*) was enhanced (Fig. 5). In keeping with this, full-length XIAP protein was maintained at high levels in LVS-infected PMNs, and appearance of a p30 calpain cleavage fragment was substantially diminished relative to controls (Fig. 7). As XIAP directly inhibits processing and activation of procaspases-9 and -3 [2,31], and both these events are significantly inhibited in *F. tularensis*-infected PMNs [15], our results are consistent with a model in which up-regulation of calpastatin and downregulation of the proteasome act in concert to prevent degradation of XIAP, which in turn inhibits caspases-9 and -3, as one mechanism to impair PMN apoptosis (Fig. 8).

Neutrophil turnover is also regulated by pro-survival signaling, and NFκB plays a central role in promoting PMN survival [2,36]. Thus, it is noteworthy that both NFκB transcription factors (*NFKB1* (p105), *NFKB2* (p100), and *RELA*) and antiapoptotic target genes (*IL1B*, *TRAF1*, *SOD2*, *GADD45B*, *CFLAR*, *TNFAIP3*, *BIRC4*, and *BIRC3*) were rapidly induced by LVS. GADD45 is of interest as it connects MAP kinase and NF B signaling pathways and can counteract FAS-stimulated cell death [37]. In addition to it effects on NF B, LVS also enhanced expression of neutrophil-specific survival factors such as *CDK2* and *CDK7* [2,29], and cytokines and chemokine genes that promote inflammation as well as PMN survival (*IL1B*, *IL1RN*, *IL6*, *OSM, PBEF1*, *CXCL1*, *CCL4, CXCR4)* [26–28]. These results suggest that the LVS-induced transcriptome may act at several levels to extend cell lifespan.

Finally, we report that *F. tularensis* also significantly affected expression of genes associated with cytosolic pattern recognition systems and inflammasome activation, with early induction of *NLRP3* and *NOD2* followed by downregulation of *AIM2, NAIP, PYCARD* and *NLRP1* (Fig. 5). Recent studies indicate that the NLRP3/ASC/capspase-1 inflammasome is functional in human neutrophils and is required for IL-1 secretion [38]. Additionally, *PYCARD* and its product ASC are strongly induced during constitutive and FAS-triggered neutrophil turnover [39], whereas polymorphisms in *NLRP3* are associated with delayed constitutive and microbe-stimulated neutrophil death [40]. Dynamic regulation of neutrophil inflammasome components by *F. tularensis* merits further study, particularly since the AIM2 and NLRP3 inflammasomes are modulated by this organism in macrophages [41,42].

In summary, the results of this study demonstrate that *F. tularensis* LVS substantially alters the human neutrophil transcriptome, including expression of genes associated with apoptosis and cell fate. Our data indicate that *F. tularensis* does not stimulate the PICD pathway, and strongly suggest that opposing effects of this organism on BAX and XIAP contribute to apoptosis inhibition. However, as the effects of *F. tularensis* are complex, it is also likely that this organism acts at multiple points to manipulate apoptotic and pro-survival pathways as a means to impair constitutive PMN turnover. Although additional studies are needed to elucidate the relative importance of the gene expression changes reported here, our data provide new insight into the molecular events that account for the ability of *F. tularensis* to alter neutrophil lifespan, and underscore the ability of systems biology approaches to advance our understanding of innate immune subversion by bacterial pathogens.

Supplementary Material

Refer to Web version on PubMed Central for supplementary material.

Acknowledgments

This work was supported in part by funds from the Public Health Service: NIH NIAID R01AI073835-05 to L.-A.H.A., a T32-AI007511 predoctoral fellowship to J.T.S., and the Intramural Research Program of the NIAID, NIH. We thank Swarup Bhattacharya of the University of Iowa Hospitals and Clinics (Iowa City, IA) for his help with data analysis.

Abbreviations

BAX	Bcl-2-associated X protein
DAVID	Database for Annotation, Visualization and Integrated Discovery
FDR	false discovery rate
GO	gene ontogeny
HBSS	Hank's buffered salt solution
KEGG	Kyoto Encyclopedia of Genes and Genomes
LVS	live vaccine strain
mAb	monoclonal antibody
MOI	multiplicity of infection
OpZ	opsonized zymosan
PCA	principal component analysis
PICD	phagocytosis-induced cell death
PMN	polymorphonuclear leukocyte
PS	phosphatidylserine
ROS	reactive oxygen species
XIAP	X-linked inhibitor of apoptosis protein

References

1. Kennedy A, DeLeo F. Neutrophil apoptosis and the resolution of infection. Immunol Res. 2009; 43:25–61. [PubMed: 19066741]
2. Geering B, Simon HU. Peculiarities of cell death mechanisms in neutrophils. Cell Death Differ. 2011; 18:1457–1469. [PubMed: 21637292]
3. Kobayashi SD, Voyich JM, Braughton KR, DeLeo FR. Down-regulation of proinflammatory capacity during apoptosis in human polymorphonuclear leukocytes. J Immunol. 2003; 170:3357–3368. [PubMed: 12626596]
4. Kobayashi SD, Voyich JM, Somerville GA, Braughton KR, Malech HL, Musser JM, DeLeo FR. An apoptosis-differentiation program in human polymorphonuclear leukocytes facilitates resolution of inflammation. J Leukoc Biol. 2003; 73:315–322. [PubMed: 12554809]
5. Kobayashi SD, DeLeo FR. Role of neutrophils in innate immunity: A systems biology-level approach. Wiley Interdiscip Rev Syst Biol Med. 2009; 1:309–333. [PubMed: 20836000]
6. Jack RM, Fearon DT. Selective synthesis of mRNA and proteins by human peripheral blood neutrophils. J Immunol. 1988; 140:4286–4293. [PubMed: 2453576]

7. Kobayashi SD, Braughton KR, Whitney AR, Voyich JM, Schwan TG, Musser JM, DeLeo FR. Bacterial pathogens modulate an apoptosis differentiation program in human neutrophils. Proc Natl Acad Sci, USA. 2003; 100:10948–10953. [PubMed: 12960399]
8. Kobayashi SD, Voyich JM, Buhl CL, Stahl RM, DeLeo FR. Global changes in gene expression by human polymorphonuclear leukocytes during receptor-mediated phagocytosis: Cell fate is regulated at the level of gene expression. Proc Natl Acad Sci U S A. 2002; 99:6901–6906. [PubMed: 11983860]
9. Watson RW, Redmond HP, Wang JH, Condron C, Bouchier-Hayes D. Neutrophils undergo apoptosis following ingestion of *Escherichia coli*. J Immunol. 1996; 156:3986–3992. [PubMed: 8621940]
10. Kobayashi SD, Voyich JM, Braughton KR, Whitney AR, Nauseef WM, Malech HL, DeLeo FR. Gene expression profiling provides insight into the pathophysiology of chronic granulomatous disease. J Immunol. 2004; 172:636–643. [PubMed: 14688376]
11. Borjesson DL, Kobayashi SD, Whitney AR, Voyich JM, Argue CM, DeLeo FR. Insights into pathogen immune evasion mechanisms: *Anaplasma phagocytophilum* fails to induce an apoptosis differentiation program in human neutrophils. J Immunol. 2005; 174:6364–6372. [PubMed: 15879137]
12. DeLeo FR. Modulation of phagocyte apoptosis by bacterial pathogens. Apoptosis. 2004; 9:399–413. [PubMed: 15192322]
13. McCaffrey RL, Allen L-AH. Pivotal advance: *Francisella tularensis* evades killing by human neutrophils via inhibition of the respiratory burst and phagosome escape. J Leukoc Biol. 2006; 80:1224–1230. [PubMed: 16908516]
14. McCaffrey RL, Schwartz JT, Lindemann SR, Moreland JG, Buchan BW, Jones BD, Allen L-AH. Multiple mechanisms of nadph oxidase inhibition by type A and type B *Francisella tularensis*. J Leukoc Biol. 2010; 88:791–805. [PubMed: 20610796]
15. Schwartz JT, Barker JH, Kaufman J, Fayram DC, McCracken JM, Allen L-AH. *Francisella tularensis* inhibits the intrinsic and extrinsic pathways to delay constitutive apoptosis and prolong human neutrophil lifespan. J Immmunol. 2012; 188:3351–3363.
16. Proctor RA, White JD, Ayala E, Canonico PG. Phagocytosis of *Francisella tularensis* by rhesus monkey peripheral leukocytes. Infect Immun. 1975; 11:146–152. [PubMed: 234911]
17. Nauseef WW. Isolation of human neutrophils from venous blood. Methods Mol Biol. 2007; 412:15–20. [PubMed: 18453102]
18. Koziel J, Maciag-Gudowska A, Mikolajczyk T, Bzowska M, Sturdevant DE, Whitney AR, Shaw LN, DeLeo FR, Potempa J. Phagocytosis of *Staphylococcus aureus* by macrophages exerts cytoprotective effects manifested by the upregulation of antiapoptotic factors. PLoS ONE. 2009; 4:e5210. [PubMed: 19381294]
19. Huang DW, Sherman BT, Lempicki RA. Systematic and integrative analysis of large gene lists using david bioinformatics resources. Nat Protoc. 2008; 4:44–57.
20. Huang DW, Sherman BT, Lempicki RA. Bioinformatics enrichment tools: Paths toward the comprehensive functional analysis of large gene lists. Nucleic Acids Res. 2009; 37:1–13. [PubMed: 19033363]
21. Gardai SJ, Whitlock BB, Xiao YQ, Bratton DB, Henson PM. Oxidants inhibit ERK/MAPK and prevent its ability to eelay neutrophil apoptosis downstream of mitochondrial changes and at the level of XIAP. J Biol chem. 2004; 279:44695–44703. [PubMed: 15292176]
22. Brach M, deVos S, Gruss H, Herrmann F. Prolongation of survival of human polymorphonuclear neutrophils by granulocyte-macrophage colony-stimulating factor is caused by inhibition of programmed cell death. Blood. 1992; 80:2920–2924. [PubMed: 1280481]
23. Hubert M, Engelen S. Robust PCA and classification in biosciences. Bioinformatics. 2004; 20:1728–1736. [PubMed: 14988110]
24. Alter O, Brown PO, Botstein D. Singular value decomposition for genome-wide expression data processing and modeling. Proc Natl Acad Sci U S A. 2000; 97:10101–10106. [PubMed: 10963673]

25. Kobayashi SD, Voyich JM, Whitney AR, DeLeo FR. Spontaneous neutrophil apoptosis and regulation of cell survival by granulocyte macrophage-colony stimulating factor. J Leukoc Biol. 2005; 78:1408–1418. [PubMed: 16204629]
26. Colotta F, Re F, Polentarutti N, Sozzani S, Mantovani A. Modulation of granulocyte survival and programmed cell death by cytokines and bacterial products. Blood. 1992; 80:2012–2020. [PubMed: 1382715]
27. Dunican AL, Leuenroth SJ, Ayala A, Simms HH. Cxc chemokine suppression of polymorphonuclear leukocyte apoptosis and preservation of function is oxidative stress independent. Shock. 2000; 13:244–250. [PubMed: 10718383]
28. Jia SH, Li Y, Parodo J, Kapus A, Fan L, Rotstein OD, Marshall JC. Pre–B cell colony–enhancing factor inhibits neutrophil apoptosis in experimental inflammation and clinical sepsis. J Clin Invest. 2004; 113:1318–1327. [PubMed: 15124023]
29. Witko-Sarsat V, Pederzoli-Ribeil M, Hirsh E, Sozzani S, Cassatella MA. Regulating neutrophil apoptosis: New players enter the game. Trends Immunol. 2011; 32:117–124. [PubMed: 21317039]
30. Altznauer F, Conus S, Cavalli A, Folkers G, Simon H-U. Calpain-1 regulates BAX and subsequent SMAC-dependent caspase-3 activation in neutrophil apoptosis. J Biol Chem. 2004; 279:5947–5957. [PubMed: 14612448]
31. Gyrd-Hansen M, Meier P. Iaps: From caspase inhibitors to modulators of NF-κB, inflammation and cancer. Nat Rev Cancer. 2010; 10:561–574. [PubMed: 20651737]
32. van Raam BJ, Drewniak A, Groenewold V, van den Berg TK, Kuijpers TW. Granulocyte colony-stimulating factor delays neutrophil apoptosis by inhibition of calpains upstream of caspase-3. Blood. 2008; 112:2046–2054. [PubMed: 18524991]
33. Yan B, Zemskova M, Holder S, Chin V, Kraft A, Koskinen PJ, Lilly M. The Pim-2 kinase phosphorylates bad on serine 112 and reverses Bad-induced cell death. J Biol Chem. 2003; 278:45358–45367. [PubMed: 12954615]
34. Knepper-Nicolai B, Savill J, Brown SB. Constitutive apoptosis in human neutrophils requires synergy between calpains and the proteasome downstream of caspases. J Biol Chem. 1998; 273:30530–30536. [PubMed: 9804822]
35. Ozaki Y, Kato T, Kitagawa M, Fujita H, Kitagawa S. Calpain inhibition delays neutrophil apoptosis via cyclic AMP-independent activation of protein kinase a and protein kinase A-mediated stabilization of Mcl-1 and X-linked inhibitor of apoptosis (XIAP). Arch Biochem Biophys. 2008; 477:227–231. [PubMed: 18647593]
36. Ward C, Chilvers ER, Lawson MF, Pryde JG, Fujihara S, Farrow SN, Haslett C, Rossi AG. NF-κB activation is a critical regulator of human granulocyte apoptosis *in vitro*. J Biol Chem. 1999; 274:4309–4318. [PubMed: 9933632]
37. Hoffman B, Liebermann DA. Gadd45 modulation of intrinsic and extrinsic stress responses in myeloid cells. J Cell Physiol. 2009; 218:26–31. [PubMed: 18780287]
38. Tamassia N, Zimmermann M, Cassatella MA. An additional piece in the puzzle of neutrophil-derived IL-1β: The NLRP3 inflammasome. Eur J Immunol. 2012; 42:565–568. [PubMed: 22488359]
39. Shiohara M, Taniguchi Si, Masumoto J, Yasui K, Koike K, Komiyama A, Sagara J. ASC, which is composed of a PYD and a CARD, is up-regulated by inflammation and apoptosis in human neutrophils. Biochem Biophys Res Commun. 2002; 293:1314–1318. [PubMed: 12054656]
40. Blomgran R, Patcha Brodin V, Verma D, Bergström I, Söderkvist P, Sjöwall C, Eriksson P, Lerm M, Stendahl O, Särndahl E. Common genetic variations in the NALP3 inflammasome are associated with delayed apoptosis of human neutrophils. PLoS ONE. 2012; 7:e31326. [PubMed: 22403613]
41. Atianand MK, Duffy EB, Shah A, Kar S, Malik M, Harton JA. *Francisella tularensis* reveals a disparity between human and mouse NLRP3 inflammasome activation. J Biol Chem. 2011; 286:39033–39042. [PubMed: 21930705]
42. Ulland TK, Buchan BW, Ketterer MR, Fernandes-Alnemri T, Meyerholz DK, Apicella MA, Alnemri ES, Jones BD, Nauseef WM, Sutterwala FS. Cutting edge: Mutation of *Francisella tularensis mviN* leads to increased macrophage absent in melanoma 2 inflammasome activation and a loss of virulence. J Immmunol. 2010; 185:2670–2674.

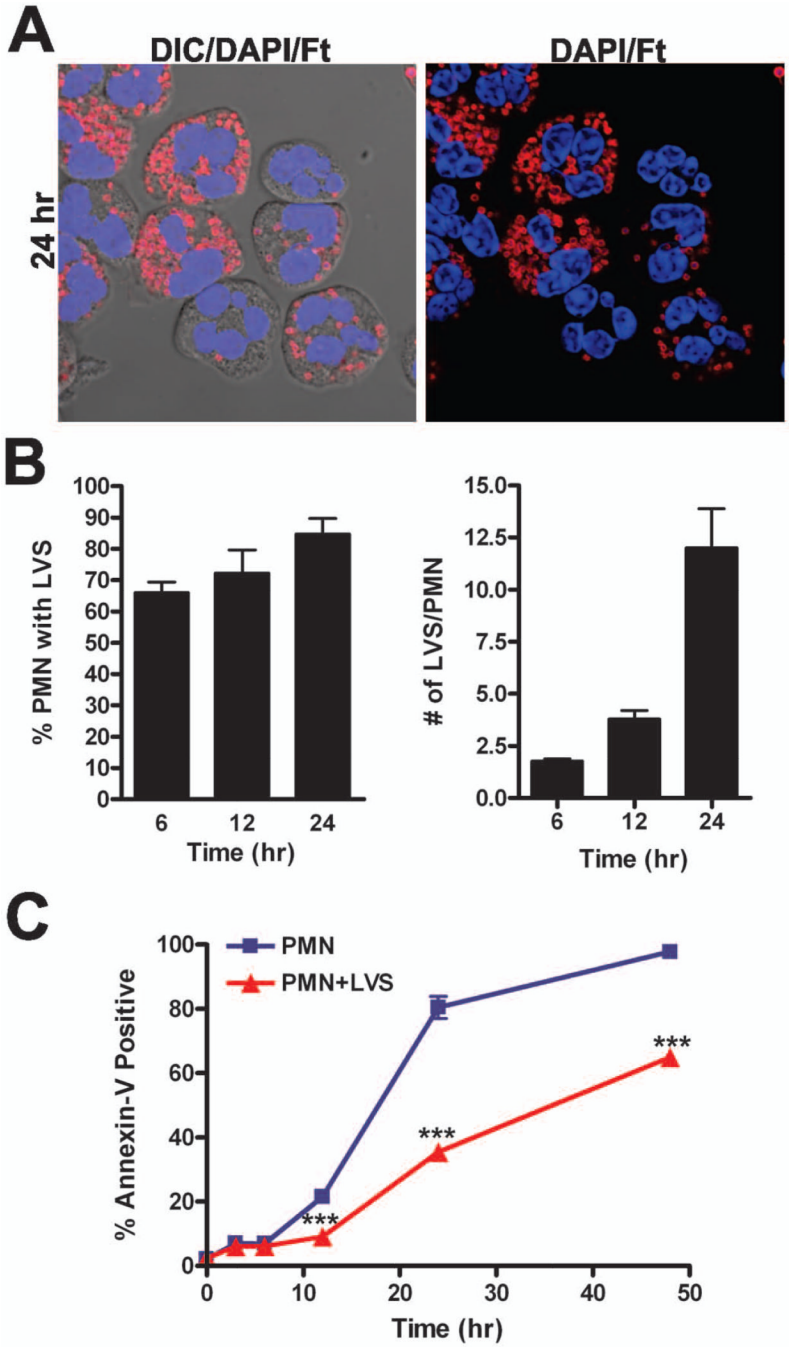

FIGURE 1.

F. tularensis LVS infects human neutrophils and impairs their spontaneous apoptosis. Neutrophils from four independent donors were infected on different days with LVS for 3–48 h at 37°C in serum-free media. ***A***, Representative confocal images of infected PMNs at 24 h. Bacteria are shown in red and PMNs were detected using differential interference contrast optics and DAPI-staining of nuclear DNA (blue). ***B***, Quantitation of infection efficiency. Graphs show the percentage of infected PMNs and bacterial load per infected cell. Pooled data are the mean ± SEM (n=4). ***C***, Apoptosis was assessed at the indicated time

points using Annexin V-FITC staining and flow cytometry. Pooled data are the mean ± SEM (n=4). ***$P < 0.001$ for control versus LVS-infected PMNs.

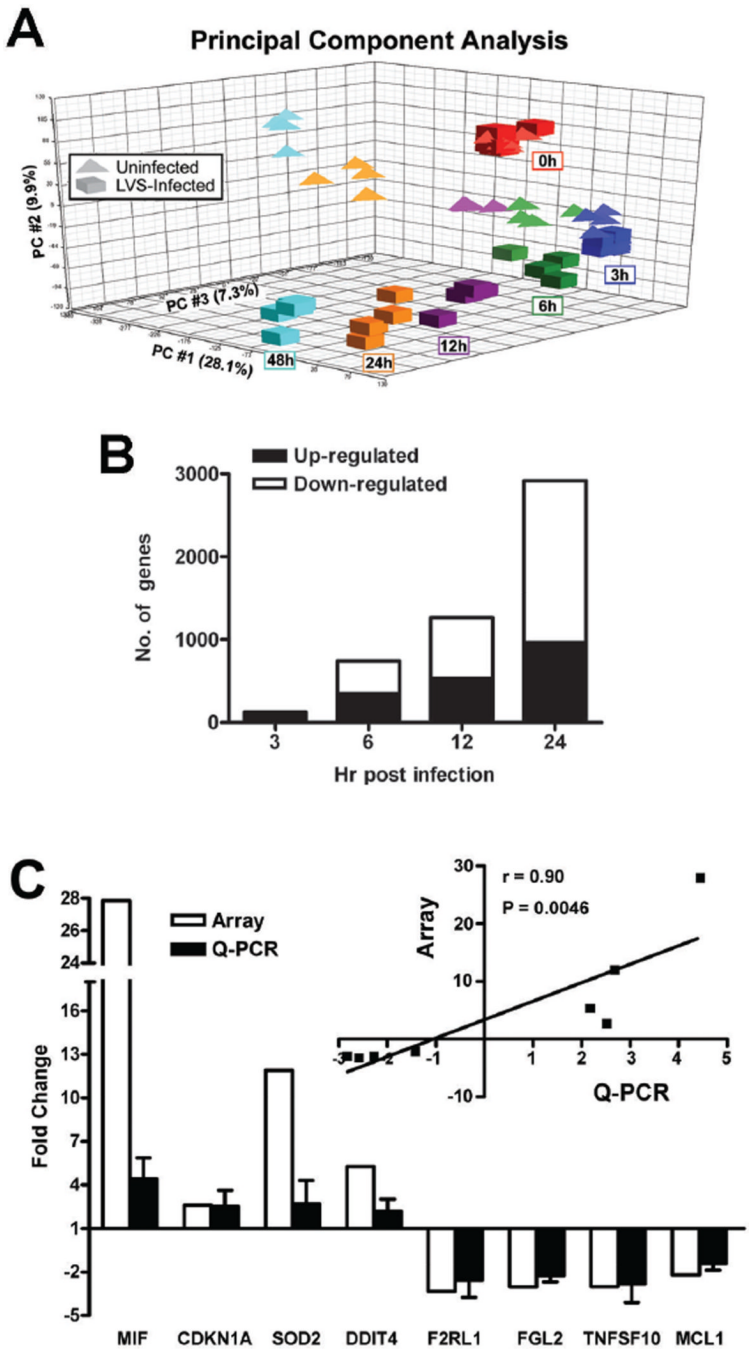

FIGURE 2.

Neutrophil gene expression is altered during *F. tularensis* infection. PMNs were left untreated or infected with LVS for 0–48 h and neutrophil gene expression was analyzed using Affymetrix human oligonucleotide microarrays. ***A***, Principal component analysis (PCA) depicts variation and clusters within the data set in three dimensions. The X-axis (PC #1) indicates the largest amount of variation (28.1%), the Y-axis (PC#2) the second largest amount of variation (9.9%), and the Z-axis (PC#3) shows all of the remaining variation (7.3%), for 45.3% variation in total. ***B***, Differentially expressed genes were categorized as up- or down-regulated and enumerated at the indicated time points. ***C***, Confirmation of the

microarray data. Differential expression of the indicated genes was quantified using real-time Q-PCR. Data shown are the mean ± SD from experiments performed using cells from three different donors. *Inset*, graph shows the strong correlation (Spearman correlation coefficient r =0.9136 and $P = 0.0046$) between the Q-PCR and microarray data.

FIGURE 3.

GeneGo pathway maps in order of significance during *F. tularensis* infection. Differentially expressed genes were analyzed by GeneGo software to identify pathways significantly altered during LVS infection of PMNs. The ten most highly significant GeneGo pathways identified are shown. *Asterisks* indicate pathways linked to apoptosis and cell survival. *Green shading* indicates pathways specifically associated with apoptosis.

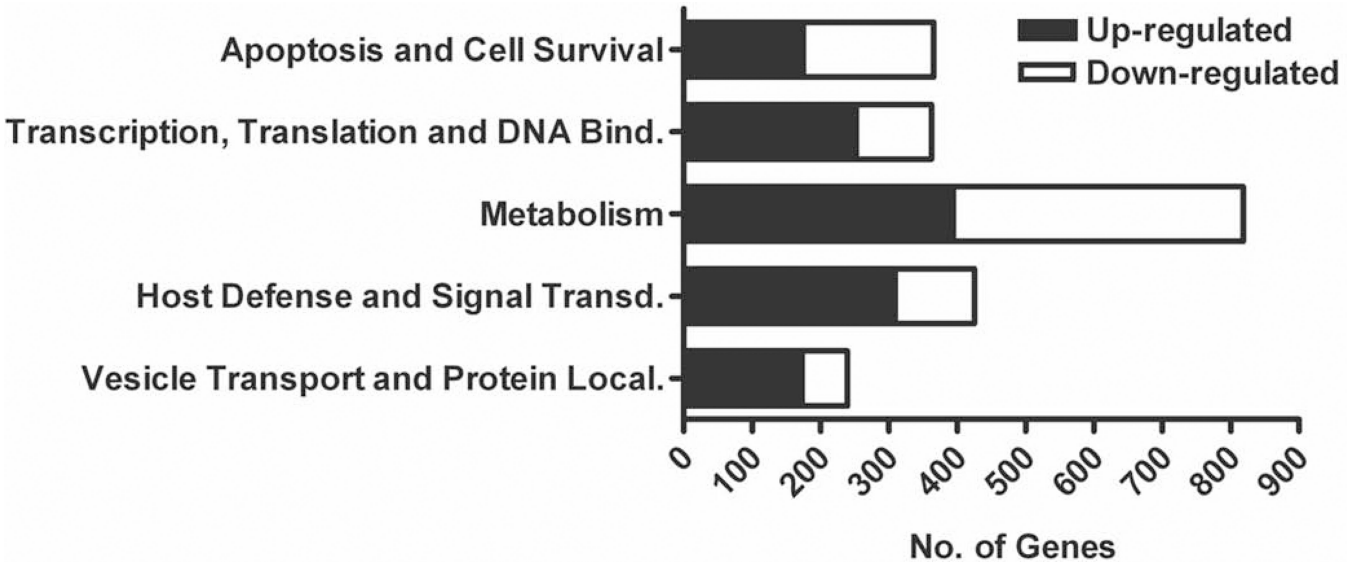

FIGURE 4.

Global alterations in neutrophil gene expression occur following infection with *F. tularensis* LVS. Genes that exhibited significant differential regulation were categorized by function using DAVID and enumerated. The numbers of up- and down-regulated neutrophil genes in each category are indicated and are based on results from all four donors.

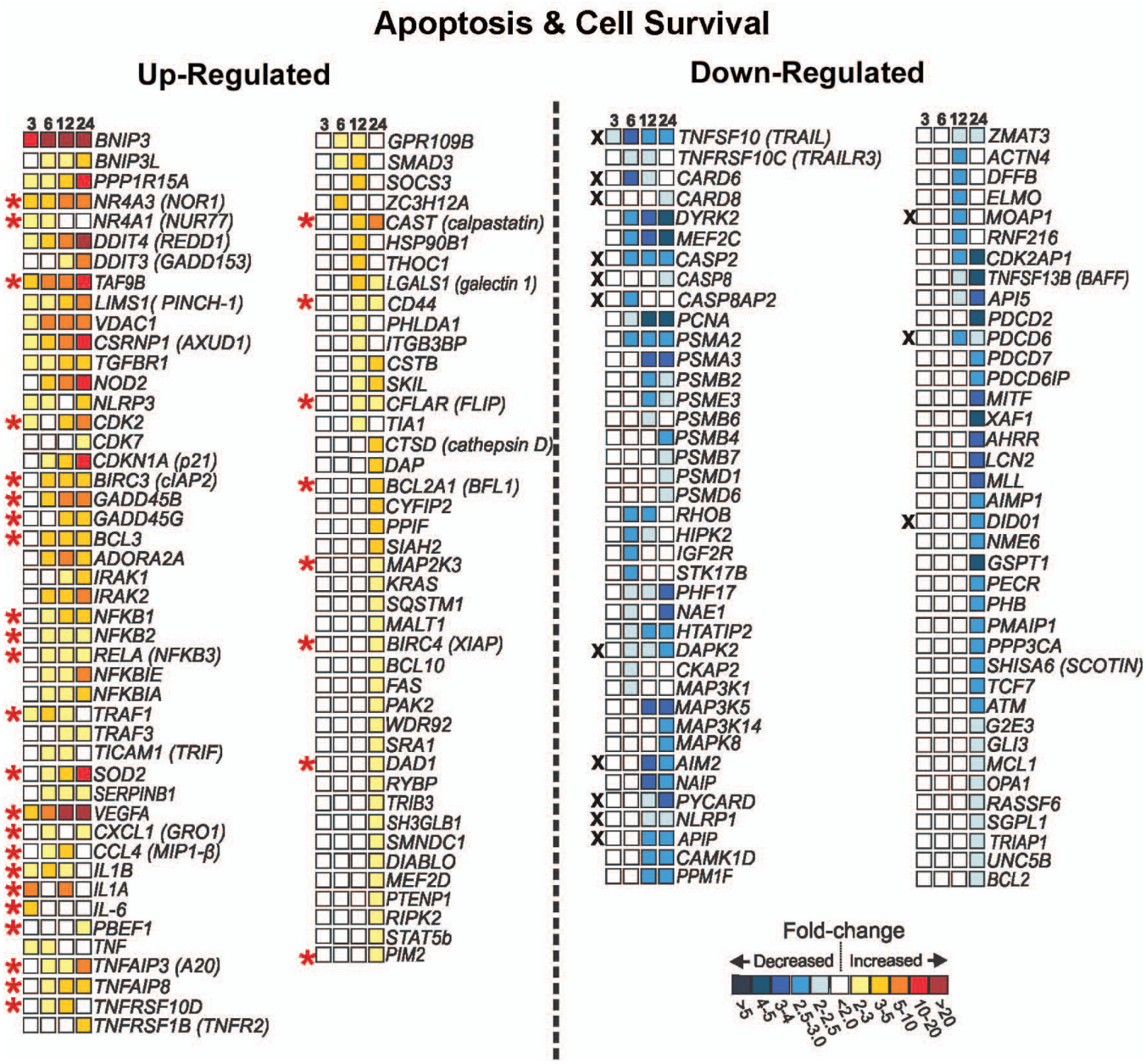

FIGURE 5.

PMN genes involved in apoptosis and cell survival are altered during infection with *F. tularensis* LVS. Differentially expressed genes (all $P<0.05$) linked to apoptosis or cell survival in previous studies are shown along with the mean fold change in expression at each time point as indicated by the color-coded scale bar. In some cases, gene names are followed by the common name for the encoded protein as a reference. Up-regulated transcripts linked to antiapoptotic or cell survival are marked with a *red asterisk*. Down-regulated transcripts associated with proapoptotic or pro-death functions are marked with a *black X*.

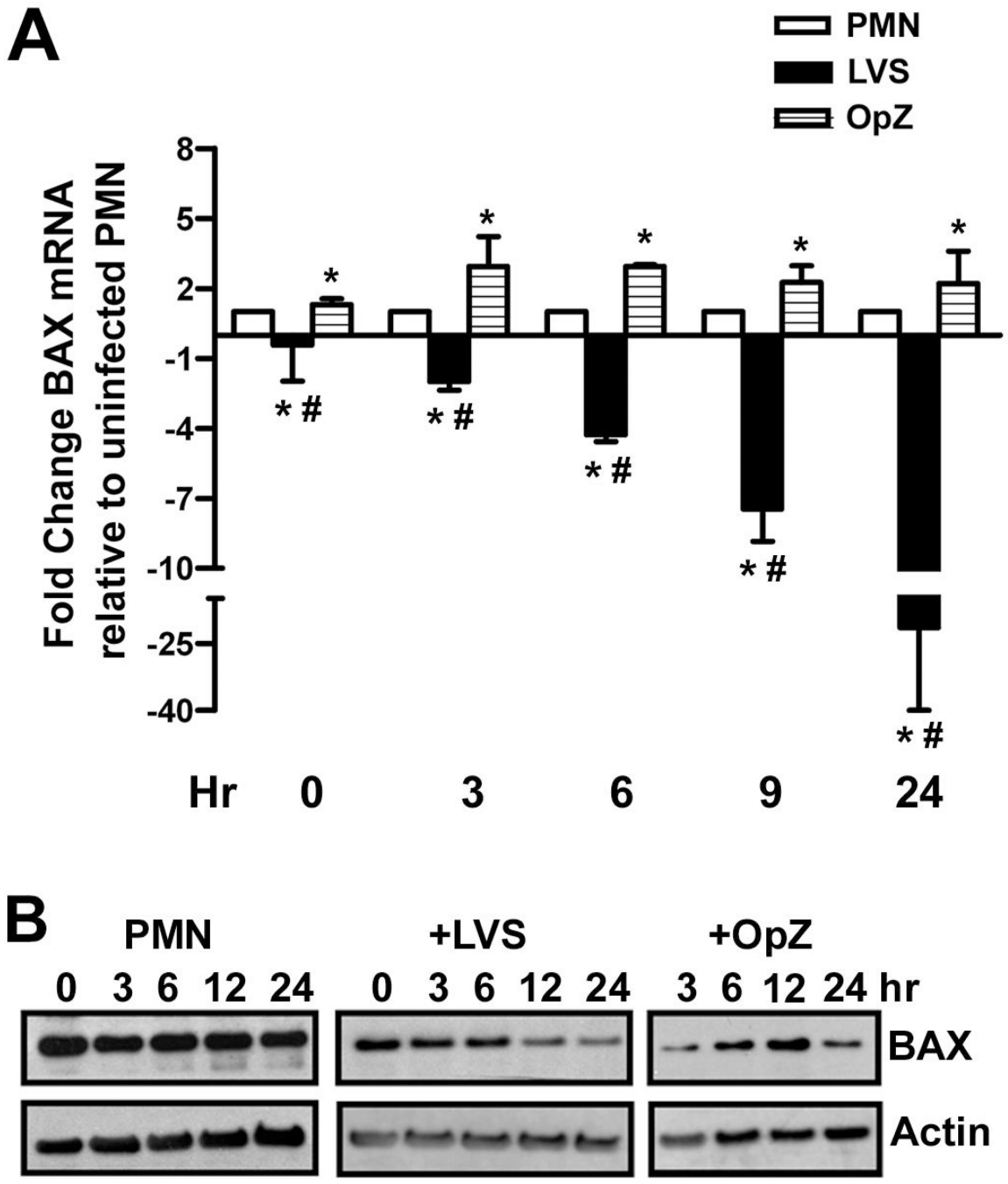

FIGURE 6.

BAX mRNA and protein are down-regulated during LVS infection. Control, LVS-infected, and OpZ-stimulated PMNs were analyzed at the indicated time points for BAX mRNA and protein. ***A***, Changes in BAX mRNA were quantified by qPCR. Data shown are the mean ± SD from two independent experiments. **P*<0.05 vs. PMN control, and #*P*<0.001 vs. OpZ by ANOVA with Tukey's post-test. ***B***, BAX protein was detected in cell lysates by immunoblotting. Actin was used as a loading control. Data shown are representative of three independent experiments.

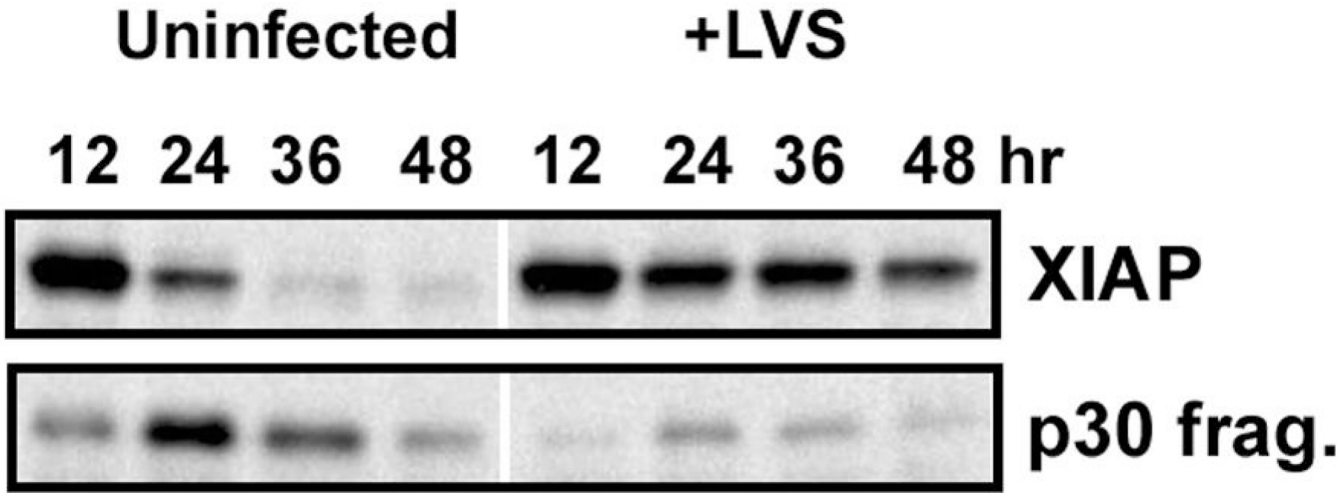

FIGURE 7.

XIAP accumulates in LVS-infected PMNs. PMNs were left untreated or infected with LVS for the indicated amount of time, and immunoblots of cell lysates were probed to detect XIAP. Full-length XIAP disappears in parallel with accumulation of a p30 XIAP fragment in PMNs undergoing constitutive apoptosis. By contrast, XIAP is maintained at high levels in LVS-infected PMNs over 48 h, and only minimal amounts of the p30 fragment were detected. The data shown are representative of three independent experiments.

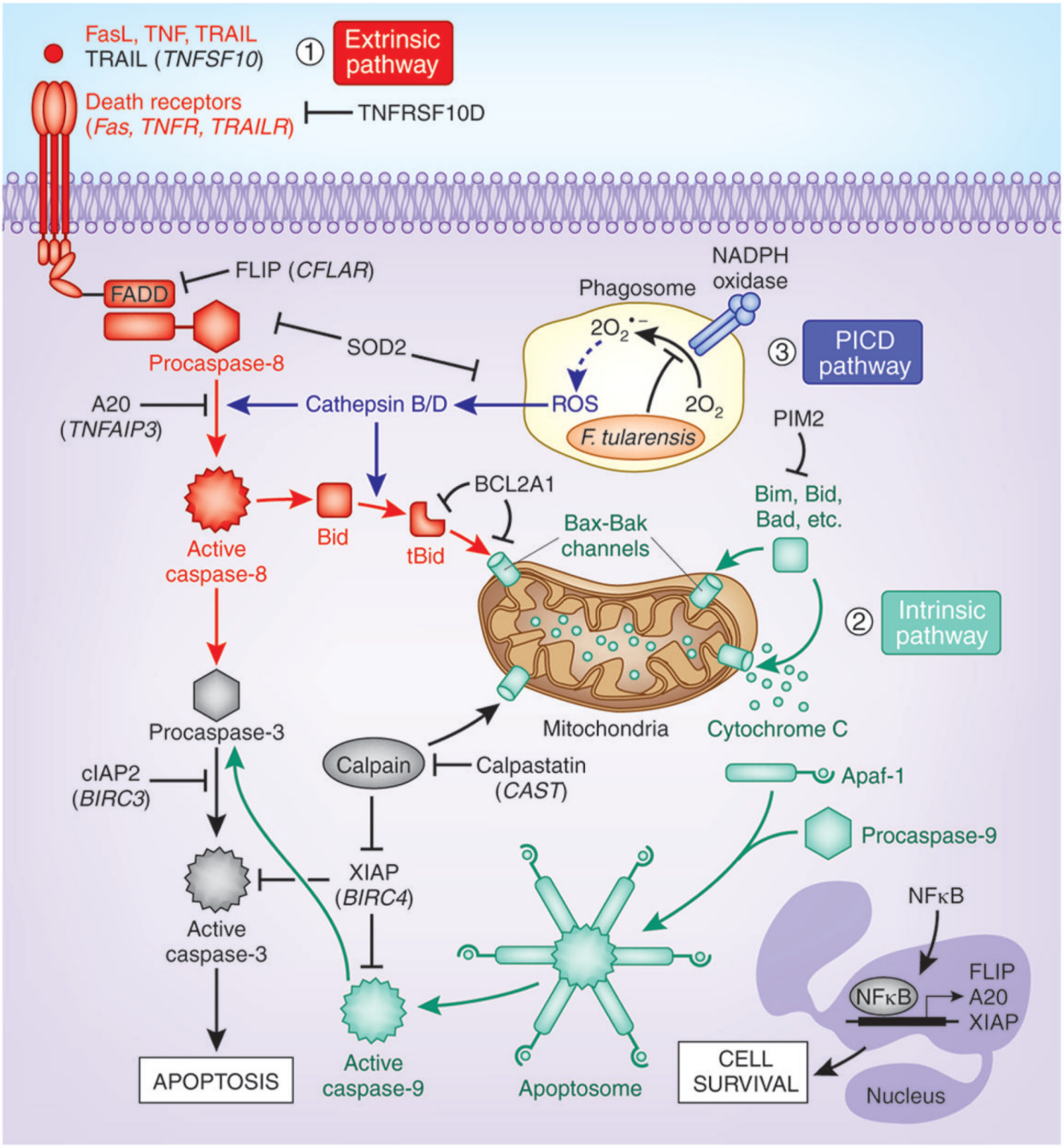

FIGURE 8.

Model of the multiple molecular mechanisms *F. tularensis* LVS may utilize to inhibit human neutrophil apoptosis. LVS modulates expression of genes that can down-regulate the extrinsic (death receptor) and intrinsic (mitochondrial) apoptotic pathways, and up-regulates expression of NF B-dependent cell survival genes. At the same time, blockade of NADPH oxidase activity at the *F. tularensis* phagosome and downregulation of BAX prevent induction of the ROS-dependent phagocytosis-induced cell death (PICD) pathway. Where protein and gene names differ, gene names are shown in parentheses.

Table I

KEGG pathways significantly enriched for differentially expressed genes during F. tularensis infection

Time Point	Pathway	Hits	*P*-value
3 hr	Glycolysis/Gluconcogcncsis	6	1.92E-04
3 hr	*MAPK signaling pathway	9	0.0027
3 hr	Prion diseases	4	0.0040
3 hr	Graft-versus-host disease	4	0.0044
3 hr	Hematopoietic cell lineage	5	0.0074
3 hr	Cytokine-cytokine receptor interaction	8	0.0085
3 hr	*NOD-like receptor signaling pathway	4	0.0195
3 hr	***Apuptosis**	**4**	**0.0465**
6 hr	Glycolysis/Gluconeogenesis	14	2.23E-06
6 hr	Fructose and mannosc metabolism	9	1.14E-04
6 hr	*NOD-like receptor signaling pathway	11	4.57E-04
6 hr	Pentose phosphate pathway	7	7.54E-04
6 hr	*Neurotrophin signaling pathway	15	0.0015
6 hr	***Apuptosis**	**12**	**0.0020**
6 hr	*MAPK signaling pathway	24	0.0025
6 hr	T cell receptor signaling pathway	13	0.0037
6 hr	*Chronic myeloid leukemia	10	0.0070
6 hr	*Pancreatic cancer	9	0.0168
6 hr	*Toil-like receptor signaling pathway	11	0.0171
6 hr	Mismatch repair	5	0.0194
12 hr	Pentose phosphate pathway	12	1.09E-06
12 hr	Glycolysis/Gluconeogenesis	16	4.53E-05
12 hr	***Apoptosis**	**18**	**3.80E-04**
12 hr	Fructose and mannose metabolism	10	9.89E-04
12 hr	*NOD-like receptor signaling pathway	13	0.0029
12 hr	*Neurotrophin signaling pathway	20	0.0037
12 hr	*Pancreatic cancer	14	0.0038
12 hr	*Chronic myeloid leukemia	14	0.0054
12 hr	Galactose metabolism	7	0.0140
12 hr	Adipocytokine signaling pathway	12	0.0152
12 hr	Starch and sucrose metabolism	9	0.0156
12 hr	Chondroitin sulfate biosynthesis	6	0.0260
12 hr	*Insulin signaling pathway	18	0.0368
12 hr	*Prostate cancer	13	0.0468
24 hr	Lysosome	36	8.35E-05
24 hr	Pentose phosphate pathway	13	1.64E-04
24 hr	B cell receptor signaling pathway	25	3.58E-04
24 hr	*Acute myeloid leukemia	20	0.0010
24 hr	Glycolysis/Gluconeogenesis	20	0.0017

Time Point	Pathway	Hits	*P*-value
24 hr	*Neurotrophin signaling pathway	33	0.0027
24 hr	*NOD-like receptor signaling pathway	19	0.0061
24 hr	*Pancreatic cancer	21	0.0069
24 hr	***Apoptosis**	**23**	**0.0150**
24 hr	Amino sugar and nucleotide sugar metabolism	14	0.0160
24 hr	T cell receptor signaling pathway	27	0.0165
24 hr	*p53 signaling pathway	19	0.0167
24 hr	*Chronic myeloid leukemia	20	0.0224
24 hr	Ubiquitin mediated proteolysis	32	0.0224

Genes that were significantly differentially expressed in control and LVS-infected neutrophils were used for pathway analysis. The KEGG pathways identified by DAVID to be significantly modulated by LVS are listed. Hits indicate the number of genes in our data set identified in the each particular KEGG pathway. *Asterisks* indicate pathways linked to apoptosis or cell survival.